ICASSP 2025 - 2025 IEEE International Conference on Acoustics, Speech and Signal Processing (ICASSP) | 979-8-3503-6874-1/25/$31.00 ©2025 IEEE | DOI: 10.1109/ICASSP49660.2025.10889351

Quantum Run-length Encoding: Optimizing Data Compression on Quantum Computers with Exponential Resource Efficiency

Jiale Zhang
College of Computer Science and Technology, Jilin University
Changchun, China
jlzhang22@mails.jlu.edu.cn

Xilong Che
College of Computer Science and Technology, Jilin University
Changchun, China
chexilong@jlu.edu.cn

Shiyong Jin
College of Intelligent Science and Engineering, Harbin Engineering University
Harbin, China
yongshijin@hrbeu.edu.cn

Kaifan Pan
Computer Network Information Center, University of Chinese Academy of Science
Beijing, China
pankf2119@mails.jlu.edu.cn

Shun Peng
College of Computer Science and Technology, Jilin University
Changchun, China
pengshun5521@mails.jlu.edu.cn

Juncheng Hu
College of Computer Science and Technology, Jilin University
Changchun, China
jchu@jlu.edu.cn

***Abstract*—Quantum computers, leveraging superposition and entanglement, offer significant qubit efficiency for data processing compared to classical systems. However, encoding classical data into quantum states, given the current limitations of quantum hardware, often results in higher runtime complexity than classical methods, thus limiting the perceived quantum advantage. Previous quantum data compression methods, primarily based on Amplitude Encoding and mixed-state systems, result in lossy data recovery and necessitate extensive preprocessing. In this work, we propose Quantum Run-Length Encoding (QRLE), a novel lossless quantum data compression method that integrates Basic Encoding with Run-Length Encoding principles. By encoding repeated data sequences with their run lengths, QRLE achieves efficient and accurate data recovery on quantum computers, while exponentially reducing both qubit costs and runtime complexity compared to existing quantum data storage models. We further explore QRLE's application in image processing, where it significantly optimizes quantum resource utilization over recent quantum image representation techniques. Experiments conducted on both quantum simulators and IBM's superconducting quantum computer validate the efficiency of QRLE and confirm its compatibility with current quantum hardware.**

I. Introduction

The rapid advancement of information technology has led to an explosive growth in data generation, creating a pressing need for more efficient data compression techniques. While classical compression algorithms, such as Huffman coding [1], Discrete Cosine Transform (DCT) [2], and Discrete Wavelet Transform (DWT) [3], have been widely used, they struggle to keep pace with this expanding data landscape. These methods require $O(N)$ bits to compress a dataset of N elements, a limitation stemming from the finite capacity of the classical bit—the smallest unit in classical computing [4]–[8]. In contrast, quantum computing, first proposed by Richard Feynman in 1982, offers promising solutions to problems that are intractable for classical computers. This potential has been demonstrated in various fields, including the quantum acceleration of classical algorithms [9], [10], quantum communication [11], quantum image processing [12]–[14], and quantum machine learning [15]–[17].

Quantum algorithms in signal processing universally require the encoding of classical data into quantum states prior to processing. While quantum computing offers the advantage of exponentially reducing qubits/bits consumption for data storage [18], optimizing quantum resource usage remains a crucial concern, especially in the Noisy Intermediate-Scale Quantum (NISQ) era [19], [20]. Despite this, research on quantum data compression remains limited, with a few initiatives exploring mixed-state encoding [21], Fourier Transform-like [22], [23] and machine learning-based compression [24]–[27].

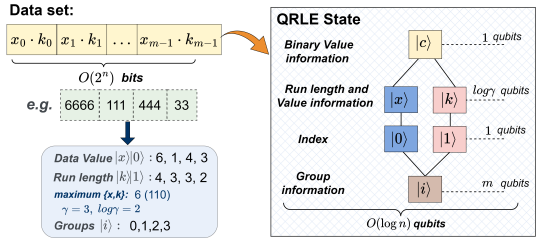

Fig. 1. Workflow of QRLE model for compressing an $N = 2^n \times 2^n$-element classical data set with m different groups into a quantum computer.

Mixed-state encoding, an adaptable variable-length coding method, exhibits considerable potential for data compression. However, its practical implementation on current quantum hardware devices remains challenging due to the requirement of handling multiple pure states, given that quantum computing hardware for pure state systems is still in the NISQ era. Methods like Fourier Transform-based and machine learning-based approaches require complex preprocessing—such as Fourier transformations and quantum neural network training—leading to significantly increased resource consumption, yet still fall short of achieving accurate data recovery. To date, lossless compression methods that simultaneously reduce qubits cost and runtime complexity on quantum computers remain unexplored.

In this paper, we propose Quantum Run-Length Encoding (QRLE), a novel quantum data compression method that combines classical Run-Length Encoding (RLE) with Basic Encoding. QRLE integrates the entanglement of run lengths and data values with their corresponding positional information, offering a lossless and resource-efficient quantum compression technique particularly suited for near-term quantum computers. We further extend our analysis to QRLE-based image processing, demonstrating a significant reduction in time complexity compared to existing models [28]–[36]. Finally, experiments on both simulators and a real superconducting quantum

Corresponding Author: Juncheng Hu, Email: jchu@jlu.edu.cn
This work is funded by the talent project of Department of Science and Technology of Jilin Province of China[Grant No.20240602106RC], and by the Central University Basic Scientific Research Fund [Grant No.2023-JCXK-04].

computer from IBM Quantum platform validate the efficacy of our QRLE model and its compatibility with current quantum hardware.

In summary, for a $N = 2^n \times 2^n$ dataset or image with a substantial number of consecutive data, the QRLE method offers the following advantages:

1) ***Qubits consumption is exponentially reduced.*** The QRLE model requires only $O(\log n)$ qubits for lossless data storage, a significant reduction compared to the $O(n)$ qubits needed by existing quantum data storage models.
2) ***The preparation process is exponentially simplified.*** The runtime complexity and quantum circuit depth for QRLE preparation are both $O(\log n \cdot n)$, a significant improvement over the $O(n \cdot 2^{2n})$ required by existing models.
3) ***Image processing operations are more flexible.*** QRLE-based image processing operations reduce runtime complexity, with some operations transitioning from $O(n^2)$ to constant time.

II. Background and related work

A. Classical Data Encoding

Depending on the required quality of reconstructed data, data compression techniques can be divided into lossless and lossy compression. Lossy data compression methods often transform data into the frequency domain such as DCT [2] and DWT [3] or are based on neural networks [5]. Notable lossless data compression methods include Huffman Encoding [1], Delta Encoding [37] and Run-Length Encoding [6]–[8], [38].

Run-Length Encoding (RLE) is a compression technique that represents consecutive occurrences of identical elements in a data sequence with a single value and a count of repetitions. It efficiently reduces data size by encoding run length of the same element, making it a widely used method for lossless compression in data and image processing. However, all the classical lossless compression methods require $O(N)$ bits/time complexity to store a dataset of N elements.

B. Quantum Data Encoding and Compression

Quantum data encoding. Quantum data encoding is generally classified into two types [39]. The first type, Basis Encoding, encodes data into the basis states of a quantum system. The second type, Amplitude Encoding, encodes data into the amplitude of quantum states. Basis Encoding allows for precise data reconstruction by leveraging the orthogonal separability theorem [18], while Amplitude Encoding is more qubit-efficient but can only recover data probabilistically and requires multiple quantum measurements.

Quantum data compression. Beyond encoding, research has extended to quantum data compression. Some studies focus on mixed-state encoding, analogous to variable-length encodings in classical computers [21]. However, mixed-state encoding remains challenging with current NISQ-era hardware, which predominantly supports pure states. Other approaches, including quantum Fourier, cosine, and wavelet transforms, or quantum neural networks for data compression [22]–[27], primarily based on Amplitude Encoding, which complicates precise data recovery and requires significant preprocessing and measurements.

Although quantum computers require only $O(\log n)$ qubits to store an $N = 2^n \times 2^n$-element set, the runtime complexity remains $O(n \cdot 2^n)$—far exceeding the classical $O(2^n)$. A resource-efficient, lossless quantum data compression method has yet to be explored.

III. Quantum Run-length Encoding

By combining the principles of classical Run-Length Encoding and Basic Encoding, the proposed Quantum Run-Length Encoding (QRLE) model comprises two entangled qubit sequences: one for the data value and its corresponding run length, $|l\rangle$, and the other for the order information of elements, $|i\rangle$, as illustrated in Figure 1.

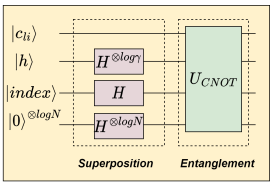

Fig. 2. The quantum circuit construction of QRLE model involves two steps: superposition through the H gate and entanglement via the U_{CNOT} gate.

Algorithm 1 QRLE compression for an N-element dataset χ with m distinct value groups

INPUT $\chi = x_0 \cdot k_0, \ldots, x_{m-1} \cdot k_{m-1}$
OUTPUT $|QRLE\rangle$
PROCEDURE
Find γ: bits required for $max\{x_i, k_i\}$, $i = 0, \ldots, m-1$;
Initialization: $|0\rangle^{log(m\cdot\gamma)+2}$;
Superposition: $\longrightarrow \sum_{h=0}^{\gamma-1}\sum_{i=0}^{m-1} |0\rangle \otimes |h\rangle\,|index\rangle\,|i\rangle$;
Entanglement: $\longrightarrow \sum_{i=0}^{m-1} |c_i\rangle\,(|x_i\rangle\,|0\rangle + |k_i\rangle\,|1\rangle)\,|i\rangle$;
MEASUREMENT
Obtain $|QRLE\rangle$
RETURN $|QRLE\rangle$

For an $N = 2^n \times 2^n$-element dataset x, with m distinct value groups, the sequence $|i\rangle$ of $logm$ qubits represents the order information for each group, where $i = 0, 1, \ldots, m-1$. Let x_i and k_i denote the data value and run length of the i-th group, respectively. The number of bits required to represent $max\{x, k\}$ in binary form is denoted by γ, and $log\gamma$ qubits are required to index the bit order of γ. An additional qubit, $|index\rangle$, is used to indicate whether the $log\gamma$ qubits store the data value x_i or the run length k_i for the i-th group. Another qubit, $|c\rangle$, encodes the binary value of x_i and k_i. Therefore, the total number of qubits required is $logm + log\gamma + 2$, and the QRLE state $|QRLE\rangle$ can be expressed as:

$$|QRLE\rangle = \frac{1}{\sqrt{2\gamma m}} \sum_{h=0}^{\gamma-1}\sum_{i=0}^{m-1} |c_{hi}\rangle\,|h\rangle\,|index\rangle\,|i\rangle\,; \tag{1}$$

$$= \frac{1}{\sqrt{2\gamma m}} \sum_{i=0}^{m-1} |c_i\rangle\,(|x_i\rangle\,|0\rangle + |k_i\rangle\,|1\rangle)\,|i\rangle\,, \tag{2}$$

where $|h\rangle$ represents the superposition state of $|x\rangle$ and $|k\rangle$.

QRLE can be extended to compress color images across the three RGB channels by adding two extra qubits, $|index_{0,1}\rangle$, as follows:

$$|\psi\rangle = \frac{1}{2\sqrt{\gamma m}} \sum_{h=0}^{\gamma-1}\sum_{i=0}^{m-1} |c_{hi}\rangle\,|h\rangle\,|index_{0,1}\rangle\,|i\rangle\,; \tag{3}$$

$$= \frac{1}{2\sqrt{\gamma m}} \sum_{i=0}^{m-1} |c_i\rangle\,(|r_i\rangle\,|00\rangle + |g_i\rangle\,|01\rangle + |b_i\rangle\,|10\rangle + |k_{li}\rangle\,|11\rangle)\,|i\rangle\,, \tag{4}$$

where $|index_{0,1}\rangle = |00\rangle$, $|01\rangle$, $|10\rangle$, and $|11\rangle$ correspond to the R, G, B channels and run length, respectively. Algorithm 1 outlines the process of compressing an N-element dataset χ with m groups using the QRLE model, while Figure 2 illustrates the quantum circuit construction. The preparation procedure of QRLE requires only H gates and U_{CNOT} gates, ensuring that the data information for each qubit is either $|0\rangle$ or $|1\rangle$, which can be accurately recovered [18].

TABLE I

RESOURCE CONSUMPTION COMPARISONS BETWEEN QRLE AND EXISTING QUANTUM DATA STORAGE MODELS FOR STORING AN $N = 2^n \times 2^n$ DATA SET.

Comparison	QRLE	Existing models
Qubits resource	$O(\log n)$	$O(n)$
Runtime complexity	$O(\log n \cdot n)$	$O(n \cdot 2^{2n})$
Quantum circuit depth	$O(\log n \cdot n)$	$O(n \cdot 2^{2n})$
Controlled qubits	$O(\log n)$	$O(n)$
Number of entangled states	$O(n)$	$O(2^n)$
Image restoration	Lossless	Lossless/Loss

IV. EXPERIMENT AND ANALYSIS

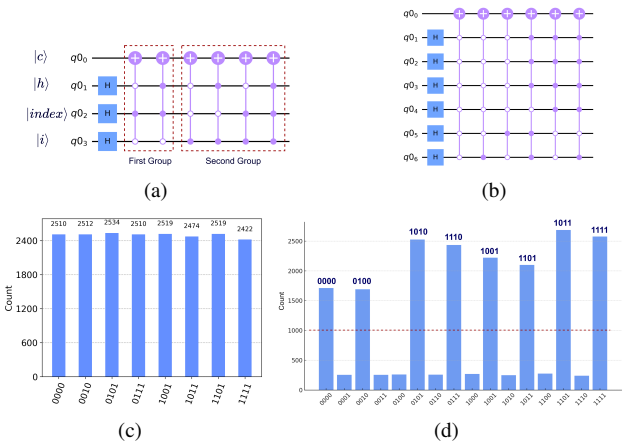

Fig. 3. (a) Quantum circuit construction of QRLE for preparing a set χ: 000,333. (b) Quantum circuit construction of BRQI for preparing set χ. (c) Simulation result of (a) using the $qasm$ simulator after 20,000 shots. (d) Experimental result of Figure 3(a) obtained from the 127-qubit superconducting quantum computer $ibm\_sherbrooke$ after 20,000 shots.

Baseline setting. Since QRLE exponentially optimizes resource consumption for compressing large consecutive data, we use all existing quantum data storage models as our baseline [28]–[36].

A. Performance analysis

Theoretical analysis. Appendix VI provides detailed analyses of qubits cost and runtime complexity for compressing an $N = 2^n \times 2^n$ set with substantial repeated data. We also focus on the other performance of QRLE such as the the number of controlled qubits and entangled states. Table I summarizes the detailed resource consumption comparison of QRLE and all the existing models [28]–[36]. The results clearly demonstrate that our QRLE model is exponentially optimized and more suitable for NISQ devices.

Case study. Beyond the theoretical analysis presented in Table I, we provide a straightforward example to further evaluate the performance of our QRLE model. Specifically, we demonstrate the compression of a simple dataset, $\chi = 000333$, using both the $qasm$ simulator and the 127-qubit superconducting quantum computer, $ibm\_sherbrooke$, on the IBM Quantum platform.

For the set $x = 000333 = 0\&3, 3\&3 = 00\&11, 11\&11$, we have $m = 2$ and $\gamma = 2$. The total number of qubits required is $\log m + \log \gamma + 2 = 4$. As shown in Figure 3(a), after applying three Hadamard gates (H), we only need to perform controlled NOT (U_{CNOT}) gates at the positions in χ where the binary values of the data and run length are 1. In the first group, 00&11, two U_{CNOT} gates are required with control bits 010 and 110. Here, the first bit represents the binary value of the run length (11), the second bit differentiates the run length, and the last qubit indicates the first group. Similarly, in the second group, two U_{CNOT} gates with control qubits 001 and 101 are required for the data value (11), while 011 and 111 are used for the run length (11). Theoretical χ compressed by QRLE on quantum computer is represented as: $|\chi\rangle = |0000\rangle + |0100\rangle + |1010\rangle + |1110\rangle + |1001\rangle + |1101\rangle + |1011\rangle + |1111\rangle$.

Figure 3(b) compares the most resource-efficient model, $MQIR$ [36], for storing χ, which is clearly much more complex than our QRLE model. Figure 3(c) presents the simulation results of the quantum circuit depicted in Figure 3(a) after 20,000 shots using the $qasm$ simulator. To validate these findings, we replicated the experiment on the IBM Quantum platform's 127-qubit superconducting quantum computer $ibm\_sherbrooke$, which has an Error Per Logical Gate (EPLG) of 1.9%, a median T1 relaxation time of 275.91 µs, and a median T2 dephasing time of 189.21 µs as depicted in Figure 3(d). Disregarding the noise in the measurement outcomes for counts below 500, the results from both $qasm$ and $ibm\_sherbrooke$ are consistent with the expected theoretical state $|\chi\rangle$.

TABLE II

COMPARISON OF TIME COMPLEXITY BETWEEN QRLE AND EXISTING QUANTUM IMAGE PRESENTATION MODELS FOR DIFFERENT IMAGE PROCESSING OPERATIONS FOR AN $N = 2^n \times 2^n$ COLOR IMAGE.

Image operations	QRLE	Existing models
Channel swapping	$\leq O(3)$	$\geq O(3)$
One channel changing	$O(\log n)$	$O(n)$
Geometric Transformation	constant ($O(\log m)$)	$O(n^2)$
Fourier Transformation	constant ($O(\log m)$)	$O(n^2)$

TABLE III

COMPARISON OF COMPRESSION PERFORMANCE BETWEEN QRLE AND RECENT LOSSLESS QUANTUM IMAGE PRESENTATION MODELS FOR A 16×16 GRAYSCALE IMAGE WITH DIFFERENT VALUES OF m AND k AS SHOWN IN FIGURE 4.

Models	Year	Qubits	Time complexity
OCQR [33]	2018	16	$\approx 16,400$
QRCI [40]	2019	12	$\approx 22,539$
MQIR [36]	2021	13	$\approx 22,539$
QRLE-(a)	/	**6**	**≈165**
QRLE-(b)	/	**7**	**≈390**
QRLE-(c)	/	**6**	**≈ 165**
QRLE-(d)	/	13	$\approx 27,904$

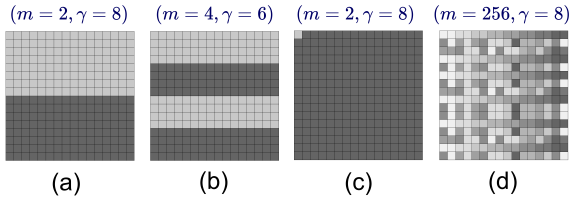

Fig. 4. Four 16×16 Grayscale images with different values of m and k.

B. Subsequent image operations

Theoretical analysis. Subsequent basic color image processing operations on QRLE image are available with lower runtime complexity, which are challenging to achieve on classical computers when an image is compressed. Leveraging the unique attributes of Run-length Encoding, QRLE image processing can operate in groups, enhancing flexibility and efficiency compared to exiting models. Due to space limitations, we omit the detailed derivations of all the available image operations on QRLE image while instead presenting a conclusion of

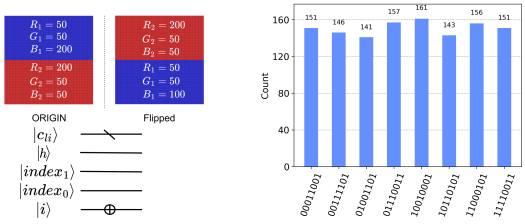

(a) (b)

Fig. 5. (a) Horizontal flipping operation on a $2^5 \times 2^5$ color image with two groups and its quantum circuit construction with only one X gate. (b) Simulation result of (a) by the $qasm$ simulator within 2,0000 shots.

basic image operations as shown in Table II.

Case study. As depicted in Figure 5(a), we use a $2^5 \times 2^5$ color image with detailed color values and $m = 2$ groups to showcase an example of Geometric Transformation on a QRLE image: horizontal flipping. The original image $|\psi\rangle$ is expressed as:

$$|1\rangle (|0001\rangle |00\rangle + |0100\rangle |01\rangle + |0101\rangle |10\rangle + |1001\rangle |11\rangle) |0\rangle + |1\rangle (|0011\rangle |00\rangle + |0110\rangle |01\rangle + |0111\rangle |10\rangle + |1001\rangle |11\rangle) |1\rangle ,$$

and the flipped image $|\psi_1\rangle$ is:

$$|1\rangle (|0001\rangle |00\rangle + |0100\rangle |01\rangle + |0101\rangle |10\rangle + |1001\rangle |11\rangle) |1\rangle + |1\rangle (|0011\rangle |00\rangle + |0110\rangle |01\rangle + |0111\rangle |10\rangle + |1001\rangle |11\rangle) |0\rangle .$$

As shown in Table II, the runtime complexity of Geometric Transformations is constant. For $m = 2$, the horizontal flip operation requires only one quantum NOT gate (X). Figure 5(b) presents the results from the $qasm$ simulator after 20,000 shots on the IBM Quantum platform, aligning with the theoretical flipped image state $|\psi_1\rangle$, confirming the correctness and high efficiency of the QRLE model in image processing operations.

We further evaluate the compression performance of QRLE on grayscale images with various m and k values, as shown in Figure 4. The results are presented in Table III, comparing QRLE with recent lossless quantum data storage models: OCQR [33], QRCI [40] and MQIR [36]. Similar to classical Run-Length Encoding, QRLE demonstrates superior compression performance when handling large volumes of sequentially identical data, as shown in cases (a), (b), and (c) in Table III. In scenarios with no consecutive identical values, QRLE's performance is comparable to existing models, as demonstrated in case (d) in Table III and analyzed in Appendix VI-B.

V. Conclusion

In conclusion, our paper presents the pioneering design and implementation of Run-length Encoding on quantum computers (QRLE). Similar to classical Run-length Encoding, QRLE excels in compressing consecutive identical data. Compared to existing models, QRLE exponentially reduces qubit consumption and runtime complexity, making it well-suited for NISQ devices. Moreover, QRLE demonstrates its potential in quantum image processing, enabling image operations with lower runtime complexity. Experiments on both simulators and a real superconducting quantum computer from the IBM Quantum platform validate the correctness and efficacy of our QRLE model. Future work will explore QRLE's applications in quantum machine learning, particularly focusing on optimizing resource efficiency in quantum neural network training.

VI. Appendix

A. Qubits cost of QRLE

Section III demonstrates that the total qubits required for QRLE to compress an $N = 2^n \times 2^n$ data set with m different groups are $\log m + \log \gamma + 2$, where $\log \gamma$ is the number of qubits required for representing data value and run length. Like the classical Run-length Encoding, QRLE achieves efficient compression performance when processing large amounts of sequential data on quantum computers. In this optimal case, run length $k \gg$ data value x and m is regarded as constant. Therefore, the required qubits for QRLE are primarily depended on γ. While γ represents the bits required for $max\{x, k\}$ in binary form and $k \leq 2^n \times 2^n$, then $\gamma \leq 2n$ and $\log \gamma \leq \log 2n$, which results in $O(\log n)$ qubits consumption for QRLE models.

B. Runtime complexity and quantum depth of QRLE

For compressing a $N = 2^n \times 2^n$-element dataset with substantial consecutive repeating data, the primary workflow for preparing a QRLE state is divided into two steps as shown in Figure 2.

At the beginning, the initial state of the quantum system is initialized as $|\psi_0\rangle = |0\rangle^{\otimes \log m + \log \gamma + 2}$, where γ is the number of bits required for $max\{x, k\}$, x the different data value, k the run length and m the different groups.

step1: Superposition. We use two important single quantum gates I and H to complete the construction of this quantum operation as $U_1 = I \otimes H^{\otimes \log m + \log \gamma + 1}$. Equation (5) illustrates the quantum transformation from the initial state $|\psi_0\rangle$ to the middle state $|\psi_1\rangle$ through the quantum operator U_1.

$$|\psi_1\rangle = U_1 |\psi_0\rangle = \frac{1}{\sqrt{2\gamma m}} \sum_{h=0}^{\gamma-1} \sum_{i=0}^{m-1} |0\rangle \otimes |h\rangle |i\rangle \quad (5)$$

step2: Entanglement. m sub-operation A_i encodes the data value x_i and run length k_i for the $i-th$ group. Each A_i is a $\log m + \log \gamma + 1$-U_{CNOT} gate so the quantum operator of ***step2***, U_2 can be expressed as $U_2 = \prod_{i=0}^{m-1} A_i$. Then the function of U_2 of step2 is described as follows:

$$U_2 |\psi_1\rangle = \frac{1}{\sqrt{2\gamma m}} \sum_{h=0}^{\gamma-1} \sum_{i=0}^{m-1} |c_{hi}\rangle |h\rangle |index\rangle |i\rangle = |QRLE\rangle \quad (6)$$

Following the aforementioned two steps, a data set is encoded and stored in a QRLE state on a quantum computer.

Theorem 1: The overall runtime complexity and quantum circuit depth required for preparing a $N = 2^n \times 2^n$ set with a substantial number of consecutive repeating data is $O(\log n \cdot n)$.

Proof: Firstly, U_1 in ***step 1*** consists of $\log m + \log \gamma + 1$ single qubit gates which cost $O(\log m + \log \gamma + 1)$ and $O(1)$ circuit depth.

Secondly, U_2 in ***step 2*** has to set the data value and run length for all groups and consists of m sub-operations. Each sub-operation contains information storage of x and k, and the maximum number of bits of their binary information is γ. Then A_i includes $2 \cdot \gamma$ U_{CNOT} gates, where each U_{CNOT} gate with $\log m + \log \gamma + 1$ controlled-bit string can be divided into $O(\log m + \log \gamma + 1)$ single quantum gates [34]–[36] and costs runtime complexity and quantum depth of $O(\log m + \log \gamma + 1)$. For all groups, the time complexity and quantum circuit depth of ***step2*** is no more than $O(2 \cdot \gamma \cdot (\log(\gamma \cdot m) + 1) \cdot m)$. Therefore, for $\gamma \leq 2n$ and $\log \gamma \leq \log 2n$, the whole runtime complexity of compressing a $N = 2^n \times 2^n$ set with m different groups into a QRLE state is no more than $O(2 \cdot \gamma \cdot (\log(\gamma \cdot m) + 1) \cdot m + \log(\gamma \cdot m) + 1) \approx O(\log n \cdot n)$. Additionally, the quantum depth is also $O(2 \cdot \gamma \cdot (\log(\gamma \cdot m) + 1) \cdot m + 1) \approx O(\log n \cdot n)$.

Notably, when the dataset lacks a significant amount of continuous data, the parameter γ becomes very small and can be approximately treated as a constant. In such cases, when $m \approx 2^n \times 2^n$, the required number of qubits increases to $O(n)$, and the runtime complexity grows to $O(n \cdot 2^n)$, which aligns with the performance of existing quantum models [31]–[36].

References

[1] A. Moffat, "Huffman coding," *ACM Computing Surveys (CSUR)*, vol. 52, no. 4, pp. 1–35, 2019.

[2] A. B. Watson *et al.*, "Image compression using the discrete cosine transform," *Mathematica journal*, vol. 4, no. 1, p. 81, 1994.

[3] T. Edwards, "Discrete wavelet transforms: Theory and implementation," *Universidad de*, vol. 1991, pp. 28–35, 1991.

[4] K. Rana and S. Thakur, "Data compression algorithm for computer vision applications: A survey," in *2017 International Conference on Computing, Communication and Automation (ICCCA)*. IEEE, 2017, pp. 1214–1219.

[5] L. Deng, G. Li, S. Han, L. Shi, and Y. Xie, "Model compression and hardware acceleration for neural networks: A comprehensive survey," *Proceedings of the IEEE*, vol. 108, no. 4, pp. 485–532, 2020.

[6] Z. Hong, T. Yang, X. Tong, Y. Zhang, S. Jiang, R. Zhou, Y. Han, J. Wang, S. Yang, and S. Liu, "Multi-scale ship detection from sar and optical imagery via a more accurate yolov3," *IEEE Journal of Selected Topics in Applied Earth Observations and Remote Sensing*, vol. 14, pp. 6083–6101, 2021.

[7] Z. Hao, Z. Wang, D. Bai, B. Tao, X. Tong, and B. Chen, "Intelligent detection of steel defects based on improved split attention networks," *Frontiers in Bioengineering and Biotechnology*, vol. 9, p. 810876, 2022.

[8] C. Wang, R. L. Chen, and L. Gu, "Improving performance of virtual machine covert timing channel through optimized run-length encoding," *Journal of Computer Science and Technology*, vol. 38, no. 4, pp. 793–806, 2023.

[9] P. W. Shor, "Algorithms for quantum computation: discrete logarithms and factoring," in *Proceedings 35th annual symposium on foundations of computer science*. Ieee, 1994, pp. 124–134.

[10] L. K. Grover, "A fast quantum mechanical algorithm for database search," in *Proceedings of the twenty-eighth annual ACM symposium on Theory of computing*, 1996, pp. 212–219.

[11] Y.-A. Chen, Q. Zhang, T.-Y. Chen, W.-Q. Cai, S.-K. Liao, J. Zhang, K. Chen, J. Yin, J.-G. Ren, Z. Chen *et al.*, "An integrated space-to-ground quantum communication network over 4,600 kilometres," *Nature*, vol. 589, no. 7841, pp. 214–219, 2021.

[12] Z. Wang, M. Xu, and Y. Zhang, "Review of quantum image processing," *Archives of Computational Methods in Engineering*, vol. 29, no. 2, pp. 737–761, 2022.

[13] D. Silver, T. Patel, A. Ranjan, H. Gandhi, W. Cutler, and D. Tiwari, "Sliq: quantum image similarity networks on noisy quantum computers," in *Proceedings of the AAAI Conference on Artificial Intelligence*, vol. 37, no. 8, 2023, pp. 9846–9854.

[14] H. Pan, X. Zhu, S. F. Atici, and A. Cetin, "A hybrid quantum-classical approach based on the hadamard transform for the convolutional layer," in *International Conference on Machine Learning*. PMLR, 2023, pp. 26 891–26 903.

[15] G. Anil, V. Vinod, and A. Narayan, "Generating universal adversarial perturbations for quantum classifiers," in *Proceedings of the AAAI Conference on Artificial Intelligence*, vol. 38, no. 10, 2024, pp. 10 891–10 899.

[16] T. Wang, H.-H. Tseng, and S. Yoo, "Quantum federated learning with quantum networks," in *ICASSP 2024-2024 IEEE International Conference on Acoustics, Speech and Signal Processing (ICASSP)*. IEEE, 2024, pp. 13 401–13 405.

[17] X. Ye, G. Yan, and J. Yan, "Vqne: Variational quantum network embedding with application to network alignment," in *Proceedings of the 29th ACM SIGKDD Conference on Knowledge Discovery and Data Mining*, 2023, pp. 3105–3115.

[18] M. A. Nielsen and I. L. Chuang, *Quantum computation and quantum information*. Cambridge university press, 2010.

[19] L. Clinton, J. Bausch, and T. Cubitt, "Hamiltonian simulation algorithms for near-term quantum hardware," *Nature communications*, vol. 12, no. 1, p. 4989, 2021.

[20] J. Preskill, "Quantum computing in the nisq era and beyond," *Quantum*, vol. 2, p. 79, 2018.

[21] Z. B. Khanian and A. Winter, "General mixed-state quantum data compression with and without entanglement assistance," *IEEE Transactions on Information Theory*, vol. 68, no. 5, pp. 3130–3138, 2022.

[22] C.-Y. Pang, R.-G. Zhou, B.-Q. Hu, W. Hu, and A. El-Rafei, "Signal and image compression using quantum discrete cosine transform," *Information Sciences*, vol. 473, pp. 121–141, 2019.

[23] M. E. Haque, M. Paul, A. Ulhaq, and T. Debnath, "Advanced quantum image representation and compression using a dct-efrqi approach," *Scientific Reports*, vol. 13, no. 1, p. 4129, 2023.

[24] C.-H. Yu, F. Gao, S. Lin, and J. Wang, "Quantum data compression by principal component analysis," *Quantum Information Processing*, vol. 18, pp. 1–20, 2019.

[25] A. Pepper, N. Tischler, and G. J. Pryde, "Experimental realization of a quantum autoencoder: The compression of qutrits via machine learning," *Physical review letters*, vol. 122, no. 6, p. 060501, 2019.

[26] C.-J. Huang, H. Ma, Q. Yin, J.-F. Tang, D. Dong, C. Chen, G.-Y. Xiang, C.-F. Li, and G.-C. Guo, "Realization of a quantum autoencoder for lossless compression of quantum data," *Physical Review A*, vol. 102, no. 3, p. 032412, 2020.

[27] R. Dilip, Y.-J. Liu, A. Smith, and F. Pollmann, "Data compression for quantum machine learning," *Physical Review Research*, vol. 4, no. 4, p. 043007, 2022.

[28] P. Q. Le, F. Dong, and K. Hirota, "A flexible representation of quantum images for polynomial preparation, image compression, and processing operations," *Quantum Information Processing*, vol. 10, pp. 63–84, 2011.

[29] G.-L. Chen, X.-H. Song, S. E. Venegas-Andraca, and A. A. Abd El-Latif, "Qirhsi: Novel quantum image representation based on hsi color space model," *Quantum Information Processing*, vol. 21, no. 1, p. 5, 2022.

[30] A. Mandal, S. Banerjee, and P. K. Panigrahi, "Hybrid phase-based representation of quantum images," *International Journal of Theoretical Physics*, vol. 62, no. 6, p. 115, 2023.

[31] Y. Zhang, K. Lu, Y. Gao, and M. Wang, "Neqr: a novel enhanced quantum representation of digital images," *Quantum information processing*, vol. 12, pp. 2833–2860, 2013.

[32] J. Sang, S. Wang, and Q. Li, "A novel quantum representation of color digital images," *Quantum Information Processing*, vol. 16, no. 2, p. 42, 2017.

[33] Kai, Liu, Yi, Zhang, Kai, Lu, Xiaoping, Wang, Xin, and Wang, "An optimized quantum representation for color digital images," *International Journal of Theoretical Physics: A Journal of Original Research and Reviews in Theoretical Physics and Related Mathematics, Dedicated to the Unification of Physics*, 2018.

[34] H.-S. Li, X. Chen, H. Xia, Y. Liang, and Z. Zhou, "A quantum image representation based on bitplanes," *IEEE access*, vol. 6, pp. 62 396–62 404, 2018.

[35] A. Mandal, S. Banerjee, and P. K. Panigrahi, "Quantum image representation on clusters," in *2021 IEEE International Conference on Quantum Computing and Engineering (QCE)*. IEEE, 2021, pp. 89–99.

[36] H.-H. Zhu, X.-B. Chen, and Y.-X. Yang, "A multimode quantum image representation and its encryption scheme," *Quantum Information Processing*, vol. 20, no. 9, p. 315, 2021.

[37] J. C. Mogul, F. Douglis, A. Feldmann, and B. Krishnamurthy, "Potential benefits of delta encoding and data compression for http," in *Proceedings of the ACM SIGCOMM'97 conference on Applications, technologies, architectures, and protocols for computer communication*, 1997, pp. 181–194.

[38] S. Golomb, "Run-length encodings (corresp.)," *IEEE transactions on information theory*, vol. 12, no. 3, pp. 399–401, 1966.

[39] R. LaRose and B. Coyle, "Robust data encodings for quantum classifiers," *Physical Review A*, vol. 102, no. 3, p. 032420, 2020.

[40] L. Wang, Q. Ran, J. Ma, S. Yu, and L. Tan, "Qrci: A new quantum representation model of color digital images," *Optics Communications*, vol. 438, pp. 147–158, 2019.